

POSSIBLE DISINTEGRATING SHORT-PERIOD SUPER-MERCURY ORBITING KIC 12557548

S. RAPPAPORT¹, A. LEVINE², E. CHIANG³, I. EL MELLAH^{1,4}, J. JENKINS⁵, B. KALOMENI^{2,6}, M. KOTSON¹, L. NELSON⁷, L. ROUSSEAU-NEPTON⁸, AND K. TRAN¹

Draft version December 8, 2021

ABSTRACT

We report here on the discovery of stellar occultations, observed with *Kepler*, that recur periodically at 15.685 hour intervals, but which vary in depth from a maximum of 1.2% to a minimum that can be less than 0.2%. The star that is apparently being occulted is KIC 12557548, a $V = 16$ magnitude K dwarf with $T_{\text{eff},s} \simeq 4400$ K. The out-of-occultation behavior shows no evidence for ellipsoidal light variations, indicating that the mass of the orbiting object is less than $\sim 3 M_J$. Because the eclipse depths are highly variable, they cannot be due solely to transits of a single planet with a fixed size. We discuss but dismiss a scenario involving a binary giant planet whose mutual orbit plane precesses, bringing one of the planets into and out of a grazing transit. This scenario seems ruled out by the dynamical instability that would result from such a configuration. The much more likely explanation involves macroscopic particles—e.g., dust, possibly in the form of micron-sized pyroxene grains—escaping the atmosphere of a slowly disintegrating planet not much larger than Mercury in size. The planetary surface is hot enough to sublimate; the resultant silicate vapor accelerates off the planet via a Parker-type thermal wind, dragging dust grains with it. We infer a mass loss rate from the observations of order $1 M_{\oplus}/\text{Gyr}$, with a dust-to-gas ratio possibly of order unity. For our fiducial $0.1 M_{\oplus}$ planet (twice the mass of Mercury), the evaporation timescale may be ~ 0.2 Gyr. Smaller mass planets are disfavored because they evaporate still more quickly, as are larger mass planets because they have surface gravities too strong to sustain outflows with the requisite mass-loss rates. The occultation profile evinces an ingress-egress asymmetry that could reflect a comet-like dust tail trailing the planet; we present simulations of such a tail.

Subject headings: eclipses — occultations — planets and satellites: general — stars: planetary systems

1. INTRODUCTION

The *Kepler* mission has now discovered some ~ 1250 very good exoplanet candidates via planetary transits of the parent star (Borucki et al. 2011). The transit depths range from a few percent for giant gas planets to only $\lesssim 10^{-4}$ for smaller planets that are of the size of the Earth. The distribution of orbital periods for these systems is shown in Fig. 1. The bulk of the systems have periods between ~ 3 and 30 days. As observations continue to be accumulated and analyzed, the newly discovered candidates will tend to be longer period systems; the short-period end of the period distribution will change relatively slowly. There are relatively few systems with

periods below a few days, and furthermore, most of the systems shown in Fig. 1 with orbital periods less than a day are either now considered to be false positives (i.e., they are most likely associated with background blended binaries) or have not yet been followed up in the detail required for conclusive categorization (Borucki et al. 2011). The confirmed short-period planets, most of which were not discovered by *Kepler*,⁹ have orbital periods between 0.73 and 1.09 days. These orbital periods are indicated by dual arrows in Fig. 1.

The shortest planetary orbital period that has been reported is 17.8 hours (Winn et al. 2011).¹⁰ The planet 55 Cnc e, the innermost of 5 planets revolving around 55 Cnc, was discovered with ground-based optical Doppler measurements (Fischer et al. 2008; Dawson & Fabrycky 2010) and detected in transit by extensive satellite observations with the *MOST* satellite (Winn et al. 2011). Winn et al. (2011) estimate its mass and radius to be $\sim 9 M_{\oplus}$ and $2 R_{\oplus}$. Planet orbits considerably shorter than a day are, in principle, quite possible, and their detection via transits using *Kepler* should not be problematic in a signal-to-noise sense. There are at least two reasons, however, why such close-in, short-period planets have not been heretofore emphasized. First, there are many short-period stellar binaries that, when their light is highly diluted by another star within a few arc seconds

¹ 37-602B, M.I.T. Department of Physics and Kavli Institute for Astrophysics and Space Research, 70 Vassar St., Cambridge, MA, 02139; sar@mit.edu

² 37-575, M.I.T. Kavli Institute for Astrophysics and Space Research, 70 Vassar St., Cambridge, MA, 02139; aml@space.mit.edu

³ Departments of Astronomy and Earth & Planetary Science, UC Berkeley, Hearst Field Annex B-20, Berkeley CA 94720-3411; echang@astro.berkeley.edu

⁴ ENS Cachan, 61 avenue du Président Wilson, 94235 Cachan, France; ielmellah@ens-cachan.fr

⁵ SETI Institute/NASA Ames Research Center, Moffett Field, CA 94035; Jon.M.Jenkins@nasa.gov

⁶ Department of Astronomy and Space Sciences, University of Ege, 35100 Bornova-Izmir, Turkey; Department of Physics, Izmir Institute of Technology, Turkey

⁷ Department of Physics, Bishop's University, 2600 College St., Sherbrooke, QC J1M 1Z7; lnelson@ubishops.ca

⁸ Département de physique, de génie physique et d'optique Université Laval, Québec, QC G1K 7P4; laurie.r-nepton.1@ulaval.ca

⁹ Taken from the “Exoplanet Orbit Database” at <http://exoplanets.org>, produced by Jason Wright, Geoff Marcy, and the California Planet Survey consortium.

¹⁰ Only just recently an exoplanet with an even shorter orbital period, KOI 961.02, with $P_{\text{orb}} = 10.9$ hours, was reported (Muirhead et al. 2012).

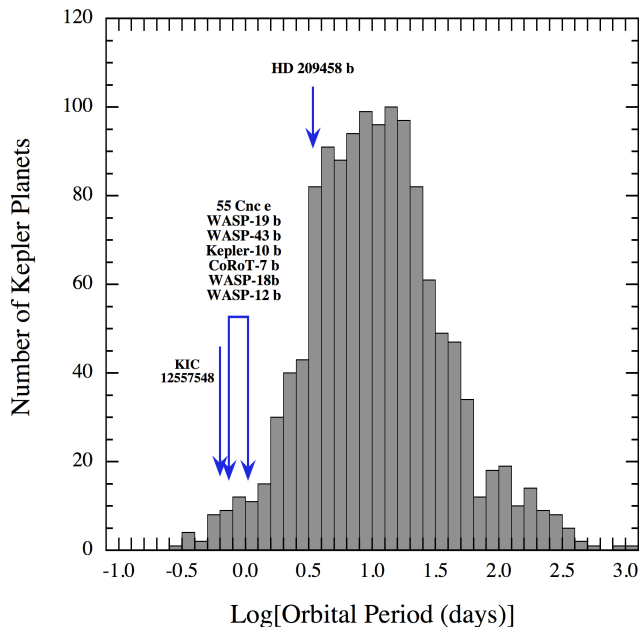


Figure 1. Distribution of orbital periods among the exoplanet candidates discovered with *Kepler*. The shorter period planets specifically named are not necessarily from the *Kepler* survey and are taken from the on-line catalog “The Exoplanet Orbit Database” (see text).

(e.g., the target star under observation by *Kepler*), are hard to distinguish from stars with transiting planets. Second, giant planets are expected to be destroyed by Roche lobe overflow if they are heated too strongly by their parent stars (Batygin, Stevenson, & Bodenheimer 2011).

With *Kepler* data, the orbital period P_{orb} of a planet about a star can be measured. If the orbit is circular, and the planet has a mass M_p much less than the mass of the parent star, then the size of the Roche lobe can be determined without knowing the mass of the parent star:

$$R_L \simeq 1.95 \left(\frac{M_p}{M_J} \right)^{1/3} \left(\frac{P_{\text{orb}}}{\text{days}} \right)^{2/3} R_J \quad (1)$$

where M_J and R_J are the mass and radius of Jupiter, respectively. Therefore, even if the planet does not evaporate because of the strong stellar radiation field, by the time a Jupiter-mass planet migrates to an orbit with $P_{\text{orb}} \lesssim 9$ hours, it will start to empty its envelope via Roche-lobe overflow.

In this work we discuss the signature of a planet in a 15.685-hour orbit about a K star. The object came to our attention via periodic occultations of the target star KIC 12557548. The term “occultation” is perhaps more appropriate than “transit” (although we will use both terms interchangeably in this paper), because of the fact that the depths of the events are highly time dependent. As we discuss in this work, the occultations are periodic to 1 part in 10^5 or more, and therefore must be due to the presence of an orbiting companion. However, the variation of the eclipse depths rules out transits by a single opaque body. More likely, we argue, the occultations are due to a stream of dust particles resulting from the slow disintegration of the planet.

In §2.2–2.5 of this work we describe detailed analyses of the *Kepler* observations of KIC 12557548 from quarters Q2 and Q3, with confirmation from the newly released quarters Q4 through Q6. In these sections we present light curves as well as power density spectra of the light curves. We also present an optical spectrum which basically confirms the spectral properties of KIC 12557548 given in the Kepler Input Catalog (KIC). In §3 we outline different plausible explanations for the variable occultation depths, including grazing transits due to a pair of planets or, more likely, obscuration by a stream of debris from a disintegrating planet. We explore in §4 the hypothesis of an occulting dust cloud in some depth. In particular, we discuss how dust can be stripped off a planet with substantial gravity. We go on to compute the approximate shape of a dust stream that has left the planet and is shaped by radiation pressure. Our findings are summarized in §5; there we also suggest future observations that may robustly establish the nature of the variable occultation depths.

2. DATA ANALYSIS

2.1. Discovery

The occultations of KIC 12557548 were discovered as part of a systematic search through the *Kepler* data base for eclipsing binaries that are not in the Prsa et al. (2011) catalog. We used publicly available quarter 2 (“Q2”) data from each of the $\sim 150,000$ *Kepler* targets to carry out a general Fourier transform search for periodicities (Kotson et al. 2012). The criteria for declaring a particular power density spectrum (PDS) as “interesting” are that (i) there is at least one peak with amplitude greater than 5 standard deviations above the local mean of the spectrum, and (ii) there is at least one harmonic or sub-harmonic of the largest peak that is at least 3 standard deviations above the local mean.

In all, we find that ~ 4800 power spectra contain interesting content, as defined above. Of these, approximately 1800 are binaries that are already in the Prsa et al. (2011) catalog, as well as some 300 binaries, mostly of the contact variety, that appear to have not made it into that catalog (Kotson et al. 2012). Most of the remaining FFTs of interest involve stars that exhibit pulsations of one sort or another.

One of the interesting power spectra contains a peak at 15.6854 hours and 15 harmonics thereof with amplitudes that decrease slowly with frequency. This is indicative of a sharp transit/eclipse/occultation which occupies only a small fraction of a cycle. The target, KIC 12557548, does not appear in either the Prsa et al. (2011) binary star catalog or the Borucki et al. (2011) planet catalog.

2.2. Light Curves

Light curves for KIC 12557548 are shown in Fig. 2. The curves shown in this figure were made by combining the raw (SAP_FLUX) light curves from quarters 2 and 3 (Q2 and Q3); before this was done the Q3 light curve was multiplied by a scale factor chosen to minimize any jump at the Q2 to Q3 boundary. Low frequency variations caused by instrumental, and possibly intrinsic source, variations were then removed by convolving the flux data with a boxcar of duration 0.65356 days (15.5854 hours) and then subtracting the convolved flux

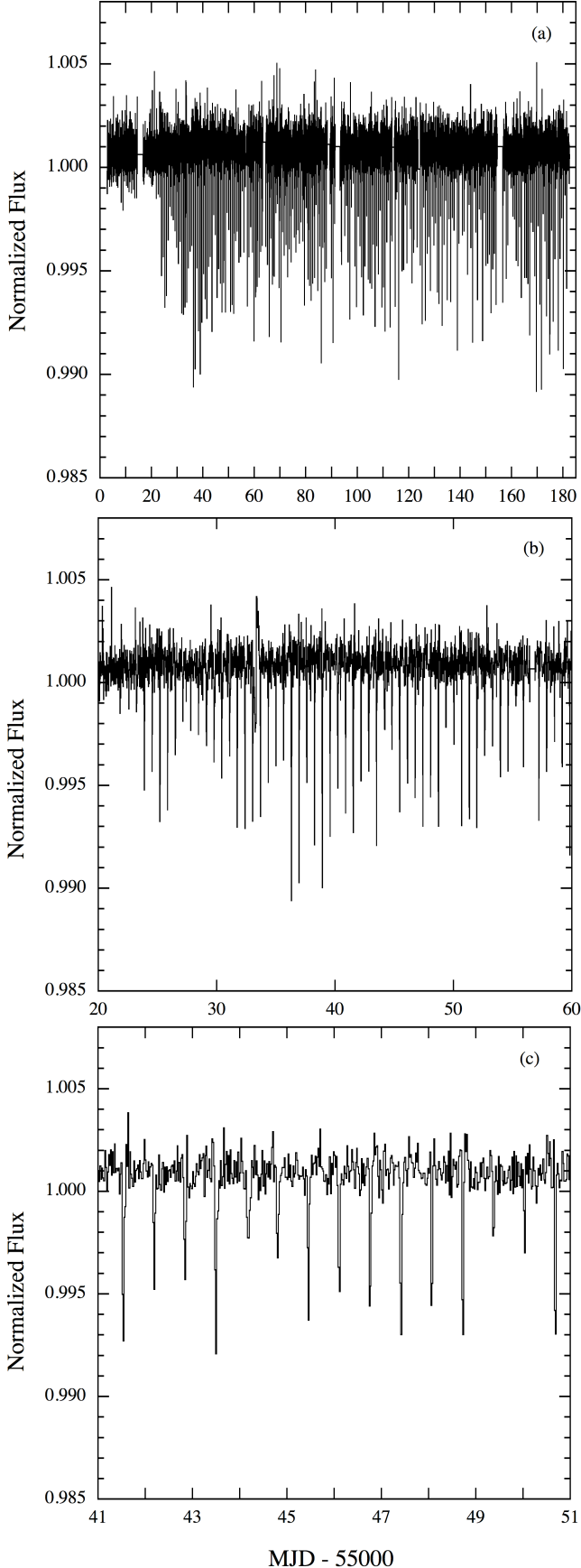


Figure 2. Light curves for KIC 12557548 spanning all of the Q2 and Q3 data sets, as well as for 40-day and 10-day segments of the Q2 data. The intrinsic Poisson fluctuations per *Kepler* sample are $\sim 0.03\%$.

curve from the pre-convolution light curve. This processing should largely preserve the actual source behavior on orbital and suborbital timescales.

Fig. 2 shows the highly variable nature of the occultations, which, in fact, have depths that render them easily seen over most of the 180 day interval, but, for the first ~ 20 days of Q2, are very small or even not noticeable. We have also checked the Q1 data and, indeed, the occultations are not apparent during the first 10 days of that quarter as well as the final 10 days. As seen in panel (c) of Fig. 2, the individual occultations vary strongly from one cycle to the next. The variable occultations persist, with a similar range in depths, throughout the following 270 days of Q4 through Q6 data.

When the data are folded about the 15.685-hour period, the results, shown in Fig. 3, further illustrate how the occultation depths vary. The largest depth is $\sim 1.2\%$, while some of the points near the middle of the occultation are depressed by no more than $\sim 0.15\%$. On the other hand, it is clear that, aside from a few individual data points within the occultation interval, almost *all* show a minimum depression in the intensity by $\sim 0.1\%$. Thus, even when the occultations are not noticeable, there still may be a small effect.

When the folded data are binned (see Fig. 3b) one can see that the average depth at the heart of the occultation is only $\sim 0.5\%$ or about half the maximum depth. There is also some evidence for a small peak in the flux at $\sim 30^\circ$ in phase before the occultation ingress, and an equally small deficit in flux just after egress. We will discuss these features briefly in Section §4.7.

The full width of the occultation, with the exception of these small features, is 0.1 of the orbital cycle. This corresponds to ~ 1.5 hours in duration, or just 3 *Kepler* long-cadence integration times. If this duration is interpreted simply as indicating the sum of the radii of the occulting “bodies” it corresponds to $(R_1 + R_2)/a \simeq 0.3$. However, if we take into account approximately the effect of the finite integration time, then $(R_1 + R_2)/a \simeq 0.24$. Note that these estimates assume, without justification, equatorial as opposed to grazing occultations.

Finally, we have fitted a constant plus a cosine of twice the orbital frequency to the folded and binned light curve, excluding the bins inside the occultation interval, i.e., at orbital phases of ± 0.085 cycles around mid occultation. We find only an upper limit of $\sim 5 \times 10^{-5}$ for the amplitude of such a feature. This limit will be discussed below in the context of setting a constraint on the mass of any body orbiting the target K star.

2.3. Fourier Search for Modulations

As a check for periodic modulations of the occultation depths for the 15.685-hour period, we carried out an FFT of the data (as shown in Fig. 2) but with the portions of the light curve away from the occultation set equal to the mean out-of-occultation intensity. The purpose of this latter step is to suppress the noise level, without sacrificing any significant fraction of the signal. The results are shown in Fig. 4. All 16 harmonics of the 15.865-hour period, out to the Nyquist limit, are clearly visible. In addition, a careful inspection of the amplitudes between the harmonics indicates some evidence for low-amplitude modulation-induced sidebands. However, at least a number of these can be reproduced in an FFT of the window

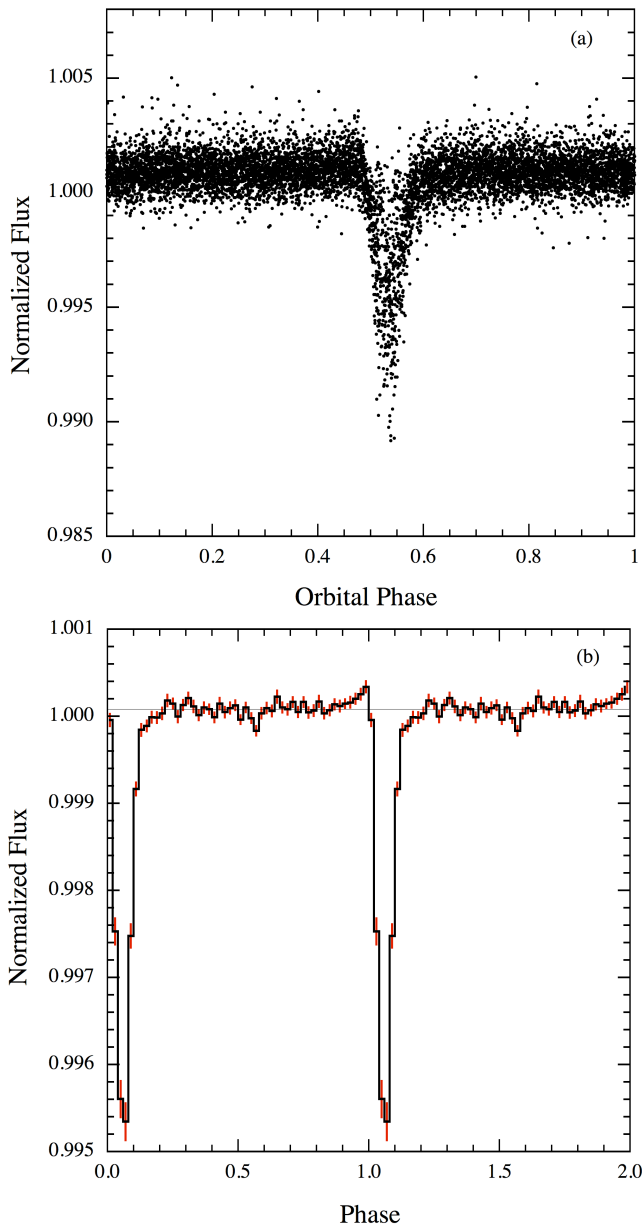


Figure 3. Folded light curves of KIC 12557548 about the 15.685-hour occultation period. Top panel – unbinned data; bottom panel – folded data averaged into 50 discrete bins. Short vertical bars on the bottom panel are the standard error of the data points within a bin.

function associated with the occultations. Thus, we find no compelling evidence for periodic modulation of the occultation depths.

2.4. Checks on the Validity of the Data

Because of the unusual exoplanet phenomenon presented in this work, we need to be especially careful to ensure that there are no spurious artifacts in the *Kepler* data for this object. In this regard, we performed a number of tests on the data.

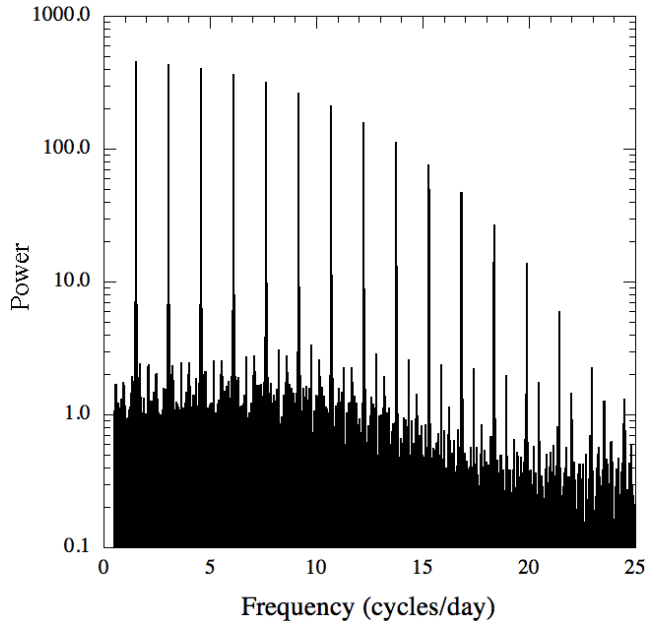


Figure 4. Power spectrum of the detrended flux data for KIC 12557548 with the out-of-occultation region set equal to the mean flux level. See text for details.

First, as mentioned above, we checked that the occultations are present in all of the quarters of released (i.e., public) data (Q1-Q6), and that the behavior of the occultations does not change abruptly across quarterly boundaries.

Second, we investigated whether the photometric variations of KIC 12557548 could be from another star or source on the sky. We examined the Digitized Sky Survey images and found that there are no especially bright stars close to KIC 12557548 whose light or transferred charge might introduce spurious signals into the data stream (i.e., none with $V < 13$ within $3'$ and none with $V \lesssim 10$ within $8'$). An examination of a *Kepler* Full Frame Image for Q1 indicates that there are no obvious stars within $\sim 38''$ (~ 10 pixels). The *Kepler* Input Catalog does list two $Kp=19$ stars located $14''$ and $17''$ from KIC 12557548 (approximately 3.5 and 4.25 pixels), but these could not be the source of the photometric variations for two reasons. (i) We checked difference images for each of Q1-Q6 and the apparent source of the photometric variations is coincident with the stellar image of KIC 12557548 (Batalha et al. 2010). Difference images compare the in-transit frames with out-of-transit frames in the neighborhood of each transit and these are averaged across all events in each quarter. (ii) Analysis of the correlation of the astrometry (brightness weighted centroids) with the photometric signature of the occultations indicates that the position of KIC 12557548 shifts by no more than ~ 0.2 millipixels in either row or column during any quarter. This indicates that there is no other offset background source that is producing the occultations within $\sim 2''$ of KIC 12557548, given the depth of the events and the brightness of KIC 12557548 (Jenkins et al. 2010).

As a further check against video crosstalk from the adjacent CCD readout channels, we examined areas on the sky located at the same row/column position on these adjacent channels, and found no stars within $11''$ of the

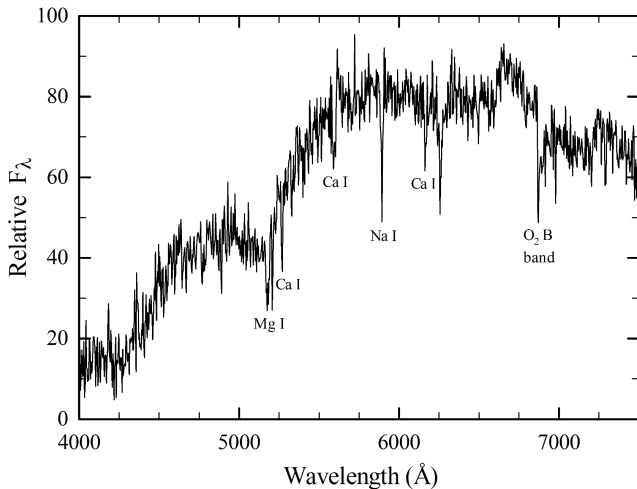


Figure 5. Optical spectrum of KIC 12557548 taken on December 16, 2011 at the OMM Observatory. The spectrum is a stack of four 15-minute exposures through ~ 1.6 air masses. The spectral features are indicative of a mid-KV star.

row/column position of KIC 12557548. The fact that the video crosstalk coefficients vary by typically 50% or more from quarter to quarter as the stars are rotated about the focal plane, and can be either negative or positive, and the fact that the photometric signatures of the occultations are consistent from quarter to quarter, provide additional confidence that it is highly unlikely that the photometric variations are due to a source on an adjacent CCD readout channel.

Third, there are no binaries in the Prsa et al. (2011) catalog or planets in the Borucki et al. (2001) catalog with periods that match that of KIC 12557548.

2.5. Optical Spectrum

KIC 12557548 is a ~ 16 th magnitude star located at RA (J2000) = $19^h 23^m 51.89^s$ and Dec (J2000) = $51^\circ 30' 17.0''$. We were able to obtain an optical spectrum of it on 2011 December 16 using the Observatoire Astronomique du Mont-Mégantic's 1.6-m telescope. Four 15-minute exposures were taken through 1.4 to 1.7 air masses soon after astronomical twilight. The spectrometer utilized the STA0520 blue CCD and a 600-line/mm grating, yielding an effective spectral resolution of 4.3 Å.

The four spectra were background subtracted, corrected for the quantum efficiency of the detector and the reflectance of the grating, corrected for Rayleigh scattering in the atmosphere, and co-added to produce the spectrum shown in Fig. 5. We did not carry out absolute flux calibrations since the purpose of this observation was simply to infer the spectral classification of the *Kepler* target and to check for any unexpected spectral features.

Despite the relatively low signal to noise ratio of this spectrum, taken under non-ideal conditions, we can clearly see the signatures of a mid-K star. Comparisons with standard stars (see, e.g., Jacoby, Hunter, & Christian 1984) indicate a spectral type of $\sim K4V$. Furthermore, we find that the equivalent width of the Na I line is

$3.6 \pm 0.4 \text{ Å}^{11}$ which is indicative of a K5-K7 star (Jaschek & Jaschek 1987). From this range of spectral types we infer $T_{\text{eff},s} \simeq 4300 \pm 250 \text{ K}$, a mass of $M_s \simeq 0.70^{+0.08}_{-0.04} M_\odot$, and a radius of $R_s \simeq 0.65^{+0.05}_{-0.04} R_\odot$, assuming that the star is close to the ZAMS. These are all quite consistent with the values listed in the KIC.

The KIC lists magnitudes of $g=16.7$, $r=15.6$, $i=15.3$, and $z=15.1$ for star 12557548. From this we estimate the V magnitude is 16.2 (Windhorst et al. 1991). If we take the absolute visual magnitude of the K star to be $+7.6$ (with $L_s \simeq 0.14 L_\odot$), and correct for an estimated $A_V \simeq 0.22$, this puts the object at a distance of about 470 pc.

3. INTERPRETATION: GENERAL REMARKS

The data analysis presented for KIC 12557548 in the previous sections reveals a highly periodic set of occultations, likely of the 16th magnitude K-star target of this particular *Kepler* field. These occultations are highly variable in depth, and are therefore very different from anything yet reported about the other several thousand transiting exoplanets (including candidates).

The remarkable stability of the occultation period strongly suggests that the occultations are due to an orbital companion to KIC 12557548. In §3.1, we constrain the separation and mass of such a companion. These constraints are quite independent of any particular model. We then outline more specific scenarios to explain the variable nature of the occultations. These are: (1) direct occultations by one planet, modulated by a second planet that causes a precession of the orbital plane of the occulting planet (§3.2), and (2) dust that emanates from a single disintegrating planet (§3.3). We consider both ideas qualitatively here, and then in §4 we elaborate on the more likely one: that the occultations are due to dust emitted directly from a planetary atmosphere.

3.1. Constraints on Separation and Mass of Orbital Companion

The regions of the light curve folded at the 15.685-hour period that are away from the occultations show no evidence—with a limiting amplitude of ~ 5 parts in 10^5 —for ellipsoidal light variations (ELVs). Since the amplitudes of ELVs are of order $\text{ELV} \simeq (R_s/a)^3 (M_p/M_s)$ (where the subscript s refers to the parent star) we can set a limit on the mass of the companion M_p (assumed $< M_s$) if we have an estimate of the companion's orbital semimajor axis a . Using the parameters for KIC 12557548 taken from the KIC, as well as our spectrum (see §2.5), we find $T_{\text{eff},s} \simeq 4400 \text{ K}$, $\log g \simeq 4.63$, and $R_s \simeq 0.65 R_\odot$. These properties all point strongly toward a mid-K star of mass $M_s \simeq 0.7 M_\odot$. The semimajor axis of a small body in a $P_{\text{orb}} = 15.7$ -hour orbit about such a star is

$$a \simeq 2.8 \left(\frac{M_s}{0.7 M_\odot} \right)^{1/3} R_\odot \simeq 0.013 \text{ AU}. \quad (2)$$

We then have a rather good estimate of R_s/a of 0.23. When this value and our upper limit on the ELV amplitude are used in the above expression for the ELV ampli-

¹¹ This is actually an upper limit to the EW because the ISM is expected to make a small contribution.

tude, we obtain a constraint on the mass of the orbiting companion of

$$M_p \lesssim 3 M_J.$$

Thus, it is unlikely that the parent star has another star, or even a brown dwarf, orbiting it at a distance of only $2.8 R_\odot$. This leaves only planetary-mass companions as the direct or indirect cause of the occultations.

3.2. Difficulties With the Dual Planet Hypothesis

From our analysis in §3.1, a planet similar to Jupiter in mass and radius could be compatible with the lack of ELVs. Such a giant planet would also generate maximum eclipse depths of $\sim 1\%$, like those observed. The challenge lies in having such a Jovian-mass planet produce highly variable transit depths.

We could try to make such a model work by supposing that the transit is grazing, and that precession of the orbital plane alters the transit geometry so that the eclipse depth varies. However, orbital precession induced either by tidal distortions or by another planet in an independent orbit generally occurs over timescales much longer than the orbital period. By contrast, the eclipse depths of KIC 12557548 vary markedly from orbit to orbit. Moreover, invoking a second planet in an attempt to force rapid variations in the planet’s trajectory across the star would probably result in detectable transit timing variations (TTVs; Agol et al. 2005; Holman & Murray 2005). But TTVs are not observed, as the orbital period is constant to ~ 1 part in 10^5 .

Another way to induce precession would be to have a second planet orbit the first in a binary planet configuration (Podsiadlowski et al. 2010). However, we have verified, using the dynamical stability criteria of Mikkola (2008, and references therein), that for the parameters of KIC 12557548, two Jupiter-sized planets cannot be in stable mutual orbit and avoid Roche lobe overflow.

3.3. Occultation by Debris from a Disintegrating Rocky Planet

Here we consider another scenario—that the occultations are produced by a much smaller, conceivably rocky planet, heated to such high temperatures that it is vaporizing. In evaporating away, it produces a debris field of dust that variably obscures up to $\sim 1\%$ of the light from the parent K star.

A purely gaseous wind emitted by a planet will not have sufficient broadband opacity to affect significantly the transit depth in the *Kepler* bandpass. For example, the hot Jupiter HD 209458b is known to emit a gaseous wind (Vidal-Madjar et al. 2003; Ben-Jaffel 2008; Linsky et al. 2010). Although this wind increases substantially the optical depth in narrow atomic absorption lines, it hardly alters the transit depth in the broadband optical. For KIC 12557548, we must consider instead that the planetary outflow contains particulates, e.g., dust. Such dust would be driven off a rocky planet so hot that it is vaporizing.

4. OBSCURATION BY DUST FROM A DISINTEGRATING SUPER-MERCURY

In this section we examine in some detail how dust emanating from a possibly rocky planet might result in

variable occultations of the parent star of up to 1.2% in depth. We discuss the size of the required dust cloud, the composition and survival requirements for the dust particles, and the required mass loss rates and implied lifetime of the planet against evaporation (§§4.1, 4.2, 4.3). The mechanism of ejecting gas and dust from a planet with non-negligible gravity is described in §4.4. We argue how dust can provide a natural explanation for the time variability of the mass loss and thereby of the variable occultation depths (§4.5). We carry out a numerical simulation of how dust, after it escapes the planet’s gravity well, is shaped into a comet-like tail, and how it might scatter radiation as well as absorb it (§§4.6, 4.7). We go on to discuss how long such a close planetary system could last under the influence of tidal drag on the orbit (§4.8). Finally, we explain why occultations by dust have not been heretofore seen in other close-in, hot, rocky planets (§4.9).

A number of these sections are necessarily speculative or involve some assumptions. We offer these simply to start the thinking process on this subject rather than to provide definitive answers.

4.1. The Underlying Planet vs. the Size of the Dust Cloud

To set the stage, we assume in what follows that the planet underlying the outflow (hereafter “KIC 1255b”) has an Earth-like composition, and has mass $M_p = 0.1 M_\oplus$ (1.8 times the mass of Mercury) and radius $R_p = 0.5 R_\oplus$. In the absence of an outflow, our nominal “super-Mercury” would produce a transit depth of at most $(R_p/R_s)^2 \approx 5 \times 10^{-5}$, consistent with our lack of detections of transits in portions of our data. The planet’s Hill sphere radius (distance from the planet to the nearest Lagrange point) is

$$R_{\text{Hill}} = \left(\frac{M_p}{3M_s} \right)^{1/3} a \simeq 1 \times 10^9 \left(\frac{M_p}{0.1 M_\oplus} \right)^{1/3} \text{ cm}. \quad (3)$$

The Hill sphere radius is smaller than R_o , defined as the characteristic size of the occulting region during the deepest eclipses (i.e., the size of the dust cloud). We adopt a nominal value for $R_o = 0.1 R_s \simeq 5 \times 10^9$ cm, which is such that if the occulting region were circular and optically thick, it would generate a transit depth of 1% , the maximum observed. From our experiments (not shown) simulating the occultation profile, we estimate that R_o could be a few times larger than our nominal choice if the occulting region were optically thin and/or the transit were not equatorial.

Why have we chosen a Mercury-like planet for our fiducial case? The reason is that to explain how dust can be ejected from the planet’s surface, we need to have the planet’s escape velocity be sufficiently low. The physics of how grains can be launched successfully from our super-Mercury is explained in §4.4. By contrast, how launch fails for hot rocky super-Earths is discussed in §4.9.

4.2. Dust Composition and Survival

Dayside planet temperatures peak at approximately

$$T_{\text{eff,p}} \simeq T_{\text{eff,s}} \sqrt{\frac{R_s}{a}} \simeq 2100 \text{ K}, \quad (4)$$

neglecting, among other effects, transport of heat from the substellar point by the atmosphere or by subsurface conduction. Such nominal temperatures are hot enough to vaporize silicates and create a high-Z atmosphere. Our model requires that this atmosphere contain refractory grains which can survive for long enough to produce an observable occultation. How much solid mass one would expect to be mixed into the atmosphere is unclear, but it is almost certainly non-zero. Rocks in the solar system (in planets, meteorites, and comets) contain agglomerations of individual grains; rocks are usually not monolithic crystals. Many of these grains are small enough (e.g., micron-sized) to be entrained with outgassing silicate vapor. One model of evaporating rocky planets posits a magma ocean at the substellar point (Schaefer & Fegley 2009; Leger et al. 2011) that would presumably dissolve all grains; but the ocean is unlikely to be global, given the strong temperature gradients on a synchronously rotating planet (or even on a close-in planet like Mercury that is not synchronously rotating). Furthermore, the silicate atmosphere can cool, both at altitude and near the day-night terminator, recondensing into particulate clouds (e.g., Schaefer & Fegley 2009; Schaefer et al. 2011; Castan & Menou 2011).

The upper mantle of the Earth is composed overwhelmingly of pyroxenes ($[\text{Mg,Fe}]\text{SiO}_3$) and olivines ($[\text{Mg,Fe}]_2\text{SiO}_4$). We might expect whatever grains to be present in the atmosphere of an evaporating sub-Earth to also consist of these minerals, at least in part. The observations of KIC 12557548 demand that grains not sublimate before they can cover up to $\sim 1\%$ of the face of the star. This requirement can be met by micron-sized grains of pyroxene, but not of olivine. In a study of grain survival times in the tails of sun-grazing comets, Kimura et al. (2002; see their Figure 4) calculated that the sublimation lifetime of an amorphous pyroxene grain having a radius $s \sim 0.2 \mu\text{m}$ is $t_{\text{sub}} \sim 3 \times 10^4 \text{ s}$ at a distance of $7.5 R_\odot$ from the Sun (equivalent to a distance of $2.8 R_\odot$ from the K star in KIC 12557548, neglecting the difference in the shape of the stellar spectrum heating the grain). Crystalline pyroxene survives for still longer, a consequence of its lower absorptivity at optical wavelengths and hence cooler temperature. By contrast, micron-sized grains of olivine ($[\text{Mg,Fe}]_2\text{SiO}_4$) vaporize in mere seconds.

A sublimation lifetime of $t_{\text{sub}} \gtrsim 3 \times 10^4 \text{ s}$, as is afforded by micron-sized pyroxene particles, is long enough for grains to travel the length of the occulting region. This travel time is on the order of

$$t_{\text{travel}} \sim \frac{R_{\text{Hill}}}{c_s} + \frac{R_o}{v} \sim 2 \times 10^4 \text{ s} \quad (5)$$

where the first term accounts for the time to travel from the planetary surface to the Hill sphere, and the second term accounts for the time to travel out to R_o . For the first leg of the journey, we have adopted a flow speed equal to the sound speed c_s in the planet's high-Z atmosphere:

$$c_s \simeq \sqrt{\frac{kT}{\mu m_H}} \simeq 0.7 \left(\frac{T}{2000 \text{ K}} \right)^{1/2} \left(\frac{30}{\mu} \right)^{1/2} \text{ km/s} \quad (6)$$

where k is Boltzmann's constant, μ is the mean molecular weight, and m_H is the mass of hydrogen. We use the

sound speed for the bulk flow speed because we believe that the grains are carried off the planetary surface by a thermal Parker-type wind, as we discuss in §4.4. For the second leg of the journey, we adopt $v \sim 10 \text{ km/s}$. This is a characteristic grain velocity once the wind is rarefied enough that dust decouples from gas, and is given by the dynamics within the Roche potential, including the Coriolis force and stellar radiation pressure (see §4.6 for details).

4.3. Mass Loss Rate and Evaporation Timescale

The mass loss rate in dust grains may be estimated as

$$\dot{M}_d \simeq \Omega \rho_d v R_o^2 \quad (7)$$

where ρ_d is the mass density in dust grains at a distance R_o from the planet, v is the outflow velocity (on scales of R_o), and Ω is the solid angle subtended by the flow as measured from the planet center. We can relate ρ_d to the optical depth through the dust flow, integrated along the line-of-sight path of length $\mathcal{R} \sim R_o$:

$$\tau \simeq \rho_d \mathcal{R} \kappa_d \sim \frac{\rho_d R_o}{\rho_b s} \quad (8)$$

where the dust opacity $\kappa_d \sim s^2/(\rho_b s^3) \sim 1/(\rho_b s)$ for grains of radius s and bulk density $\rho_b \sim 3 \text{ g cm}^{-3}$. We can also relate τ to the eclipse depth f , assuming $\tau \lesssim 1$ (we will discuss why the flow may be optically thin, or marginally so, in §4.5):

$$f \sim \frac{\tau R_o^2}{R_s^2} \sim 0.01 \left(\frac{\tau}{1} \right) \left(\frac{R_o/R_s}{0.1} \right)^2. \quad (9)$$

Combining the above three relations, we have

$$\begin{aligned} \dot{M}_d &\sim \frac{\Omega \rho_b s f R_s^2 v}{R_o} \simeq 2 \times 10^{11} \left(\frac{\Omega}{1} \right) \left(\frac{\rho_b}{3 \text{ g/cm}^3} \right) \left(\frac{s}{0.2 \mu\text{m}} \right) \\ &\times \left(\frac{f}{0.01} \right) \left(\frac{v}{10 \text{ km/s}} \right) \left(\frac{0.1}{R_o/R_s} \right) \left(\frac{R_s}{0.65 R_\odot} \right) \text{ g/s} \\ &\simeq 1 M_\oplus/\text{Gyr} \end{aligned} \quad (10)$$

where in normalizing Ω to 1 we have tried to account for the fact that the area on the planet from which dust is launched may be restricted, e.g., to the substellar region where temperatures and gas pressures are highest. As noted in §4.1, R_o could be up to a few times larger than $0.1 R_s$ (at fixed eclipse depth $f = 0.01$) if $\tau \lesssim 1$ and/or the transit is not equatorial, thereby reducing \dot{M}_d somewhat.

Gas (silicate vapor) adds to the total mass loss rate by a factor of ξ . If we assume that the mass loss mechanism acts principally on gas, and that grains are advected along by gas drag, then it seems reasonable to assume that the gas density must be at least as large as the dust density, in order for gas to carry dust: $\xi \gtrsim 2$. We will estimate this factor more quantitatively in §4.4; for now, we note that $\xi \sim 2$ falls squarely in the range of values inferred for comet tails of dust mixed with gas (Delsemme 1982; Fernandez 2005). Then the evaporation timescale for our nominal $M_p = 0.1 M_\oplus$ planet is

$$t_{\text{evap}} \sim \frac{M_p}{\mathcal{F} \xi \dot{M}_d} \sim 0.2 \left(\frac{0.3}{\mathcal{F}} \right) \left(\frac{2}{\xi} \right) \text{ Gyr} \quad (11)$$

where \mathcal{F} is the fraction of time the planet spends losing mass at the maximum rate (set by $f = 0.01$). Our estimate of t_{evap} is nominally shorter than the likely age of the star, but not by an implausibly large factor.

4.4. Ejecting Dust Grains Via a Thermal Wind

We propose that dust is ejected from KIC 1255b in a manner similar to that in comets (for a pedagogical review of comets, see Rauer 2007). Gas sublimates off a comet nucleus at essentially the sound speed, which can be dozens of times greater than the escape velocity from the nucleus. As gas atoms stream toward the cometopause—the surface of pressure balance between cometary gas and the Solar wind—they are photoionized by stellar ultraviolet photons. At the cometopause, cometary ions are rapidly picked up by the magnetic field of the Solar wind, and accelerated up to the Solar wind speed of hundreds of km/s. This explains the well-known observation that the ionized gas tails of comets are swept anti-Sunward, in the direction of the Solar wind. Dust, on the other hand, escapes the nucleus by ordinary hydrodynamic drag exerted by sublimated gas. Only the smallest dust particles, with the largest surface area to mass ratios, can be dragged off the nucleus by gas.

The main difference between a comet and KIC 1255b is the much higher surface gravity of our nominal super-Mercury. The surface escape velocity

$$v_{\text{esc,surf}} \simeq 5 \left(\frac{M_p}{0.1 M_\oplus} \right)^{1/2} \left(\frac{0.5 R_\oplus}{R_p} \right)^{1/2} \text{ km s}^{-1} \quad (12)$$

is several times higher than the local sound speed c_s . At first glance, because $v_{\text{esc,surf}}/c_s \sim 7 > 1$, it seems unlikely that gas can be driven off the surface of the planet. But in Parker-type winds (see, e.g., Lamers & Cassinelli 1999) the base of the wind can be characterized by just such values of $v_{\text{esc,surf}}/c_s$. Starting at their base, Parker-type winds accelerate by gas pressure over long distances—several planetary radii—before the bulk wind speed v formally exceeds the *local* escape velocity (as distinct from the *surface* escape velocity). For example, $v_{\text{esc,surf}}/c_s \sim 6$ at the seat of the Solar wind, i.e., the corona (e.g., Lemaire 2011). Another example is provided by the thermal winds from hot Jupiters, where $v_{\text{esc,surf}}/c_s \sim 4$ at the base of the planetary wind where stellar UV photons are absorbed and heat the upper atmosphere (e.g., Murray-Clay, Chiang, & Murray 2009). By analogy with these flows, we envision that sublimated gas from the surface of KIC 1255b can be gradually accelerated by gas pressure to speeds that eventually exceed the local escape velocity. At distances of $R_{\text{Hill}} \sim 3R_p$, we anticipate that the outflow will have attained the sonic point, so that the wind velocity will be of order c_s . Of course, this is merely an order-of-magnitude estimate which awaits refinement by detailed calculations; the actual gas velocity will be influenced also by stellar tidal gravity (see, e.g., Figure 9 of Murray-Clay et al. 2009).

How dense and fast must the gaseous outflow be to lift grains off the surface of the planet? The aerodynamic drag force on a grain must exceed the force of planetary gravity:

$$\rho_g v_g c_s s^2 \gtrsim \rho_b s^3 g \quad (13)$$

where $g \sim 400 \text{ cm s}^{-2}$ is the surface gravitational acceleration, and ρ_g and v_g are the gas density and flow velocity, respectively. For the drag force on the left-hand side we have used the Epstein (free molecular) drag law, appropriate for grains whose sizes are less than the collisional mean free path between gas molecules, and for flow velocities $v_g \lesssim c_s$ (Epstein 1924). Both of these conditions can be verified *a posteriori* to hold throughout the flow. The lift-off condition (13) implies a mass loss rate in *gas* of

$$\dot{M}_g \sim \Omega \rho_g v_g R_p^2 \gtrsim 4 \times 10^{10} \left(\frac{\Omega}{1} \right) \left(\frac{s}{0.2 \mu\text{m}} \right) \text{ g/s}. \quad (14)$$

The fact that $\min \dot{M}_g$ is comparable to \dot{M}_d as estimated in (10) justifies our claim in §4.3 that the gas-to-dust ratio may be of order unity, i.e., $\xi \sim 2$.

It is remarkable that at a maximum eclipse depth $f = 0.01$, our order-of-magnitude estimate for the total mass loss rate $\xi \dot{M}_d \sim 4 \times 10^{11} \text{ g/s}$ from our super-Mercury exceeds, by factors of a few, estimates of mass loss rates—mostly in hydrogen gas—from hot Jupiters like HD 209458b (Vidal-Madjar et al. 2003; Yelle 2004; Garcia-Munoz 2007; Murray-Clay et al. 2009; Linsky et al. 2010) and HD 189733b (Lecavelier des Etangs et al. 2010). Hot Jupiters are thought to lose mass by photoevaporation, whereby stellar X-ray and ultraviolet (XUV) radiation photoionizes, heats, and drives a thermal wind off the uppermost layers of a planetary atmosphere. Present-day mass loss rates of hot Jupiters are limited by the XUV luminosities of main-sequence solar-type stars, of order $L_{\text{XUV,s}} \sim 10^{-5} - 10^{-6} L_\odot$. By comparison, in the case of KIC 1255b, we believe that mass loss is also driven via a thermal wind—but one which is powered by the bolometric stellar luminosity, $L_s \sim 0.14 L_\odot$, which heats the entire planetary atmosphere to temperatures $T \simeq 2000 \text{ K}$, hot enough to generate an outflow from our comparatively low-gravity planet. The power required to drive our inferred mass loss rate

$$L_{\text{required}} = \frac{GM_p \xi \dot{M}_d}{R_p} \sim 6 \times 10^{22} \left(\frac{\xi}{2} \right) \left(\frac{s}{0.2 \mu\text{m}} \right) \left(\frac{\tau}{1} \right) \text{ erg/s}, \quad (15)$$

(G is the gravitational constant) is easily supplied by the total power intercepted in stellar radiation,

$$L_{\text{intercepted}} = \frac{L_s}{4\pi a^2} \cdot \pi R_p^2 \sim 4 \times 10^{26} \text{ erg/s}. \quad (16)$$

4.5. Time Variability of Mass Loss and Limiting Mass Loss Rate

The variability observed in the obscuration depths implies changes in \dot{M}_d over timescales $\lesssim P_{\text{orb}} = 15.7 \text{ hr}$. Although we cannot be quantitative, such rapid variability seems possible to accommodate within the framework of an evaporating planet. Again, a comparison with comets is instructive. As in a cometary nucleus, inhomogeneities or localized weaknesses in the planet's surface (“vents”; Jewitt 1996; Hsieh et al. 2010) may cause the planet to erupt occasionally in bursts of dust. Whatever gas is

ejected from the planet will be photoionized by the stellar radiation field and, like the gas tails of comets, interact with the magnetized stellar wind. The flow of dusty plasma along the planet's magnetotail may be subject to plasma instabilities that introduce further time variability.

These complications notwithstanding, the mass loss rate \dot{M}_d may be limited to $\sim 2 \times 10^{11} \text{ g s}^{-1}$, the value in equation (10) appropriate to an optical depth $\tau \sim 1$ (assuming all other parameters in that equation are fixed at their nominal values). This upper limit exists because if the flow became too optically thick, light from the star would not reach the planet's surface to heat it. Thus the mass loss rate may be self-limiting in a way that keeps the outflow from becoming too optically thick. One can imagine a limit cycle which alternates between a low-obscurance phase during which starlight strikes the planet's surface directly and dust proceeds to fill the planet's atmosphere, and a high-obscurance phase during which dust removal dominates over production.

4.6. Dust Stream Structure

Once dust escapes from the planet, and the gas density becomes too low to exert significant drag, the dust will be swept back into a comet-like tail by the combination of radiation pressure and Coriolis forces. The ratio of the stellar radiation pressure force on a grain to that of stellar gravity equals

$$\beta \equiv \frac{F_{\text{rad}}}{F_{\text{grav},s}} = \frac{3Q_{\text{pr}}L_s}{16\pi GcM_s\rho_b s} \simeq 0.15 \left(\frac{L_s}{0.14 L_\odot} \right) \left(\frac{0.7 M_\odot}{M_s} \right) \left(\frac{0.2 \mu\text{m}}{s} \right) \quad (17)$$

where Q_{pr} is the radiation pressure efficiency factor (see, e.g., Burns et al. 1979) and c is the speed of light. For the numerical evaluation in (17), we have used the results of Kimura et al. (2002, their Figure 2) for a spherical pyroxene particle, scaled for the luminosity and mass of our K star. The numerical result in (17) is valid only for $s \gtrsim 0.2 \mu\text{m}$ (as s decreases below $0.2 \mu\text{m}$, Q_{pr} decreases and radiation pressure is increasingly negligible; in any case such grains are unimportant because they sublimate too quickly).

We performed a simple calculation of what a dust tail might look like. Since the precise details of how dust is launched from the surface are presently unclear—they are subject, e.g., to horizontal winds on the planet that can distribute material from the substellar point to the nightside—we simply launched an isotropic flow of dust from the surface at the planet's escape speed. We used our fiducial planet parameters of $R_p = 0.5 R_\oplus$ and $M_p = 0.1 M_\oplus$, and $\beta = 0.15$. We also adopted a sublimation time for the dust of $t_{\text{sub}} = 10^4$ sec. We launched 30,000 dust particles and followed them until they sublimated. The computations were performed in a frame of reference rotating with the planet's orbit.

The results of this simulation are shown in Fig. 6. The top panel shows the projection of the dust density onto the $x - y$ plane (as viewed from the orbital pole); the bottom panel shows the projection onto the $y - z$ plane (as seen by an equatorial observer at mid transit). In

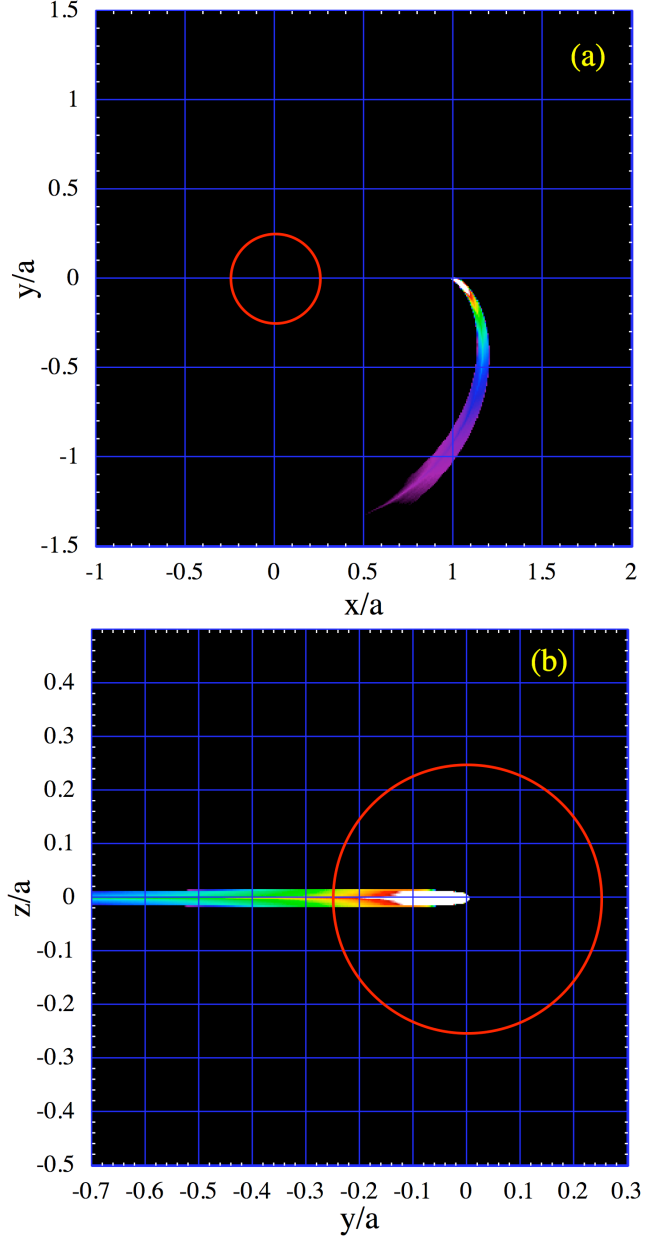


Figure 6. Simulations of dust flows from a $0.1 M_\oplus$ planet of $0.5 R_\oplus$ driven by radiation pressure from the parent star. The spatial scale is in units of the semimajor axis of the planet. The color scale is proportional to the square root of the projected density in order to enhance the dynamic range. The red circle represents the parent star.

spite of what appears to be a long dust tail (which is exaggerated by the choice of color scaling), the column density of particles is quite small at distances comparable to R_s .

We quantify this by integrating the total number of dust grains within $\pm 1/8$ of the stellar radius in height (z) as a function of distance along the dust tail (y). The result is shown in Fig. 7. We do not know what the normalization of this curve is without further observations, but this serves to show that the projected density of dust grains falls off sharply with distance from the planet. Thus, the optical depth could be somewhat greater than unity near the projected planet disk, and the net ob-

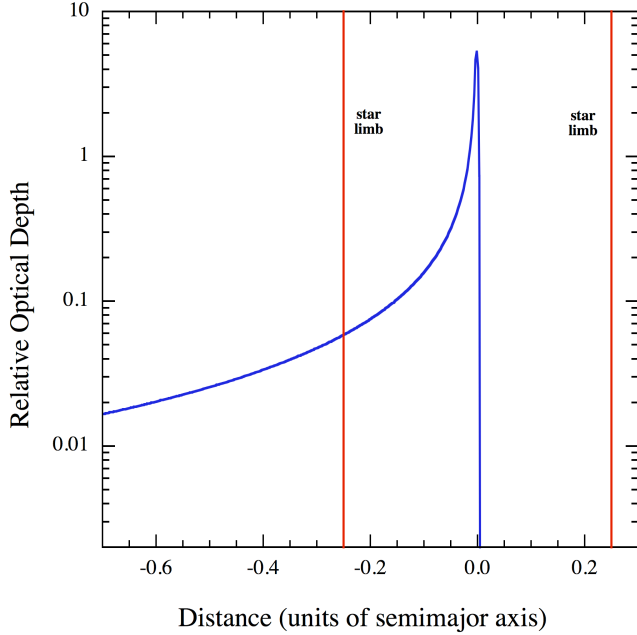


Figure 7. Relative optical depth of the simulated dust tail as a function of distance across the parent star in units of the semimajor axis. This result is derived from the simulated data used to produce Fig. 6. The vertical scale is arbitrary since otherwise we would need to know the absolute value of the optical depth near the surface of the planet.

scuration of the parent star could take values up to the maximum level of $\sim 1.2\%$ that is observed.

In summary, the dust stream geometry seems able to accommodate the occultation durations and depths. It might even be able to explain the curious ingress-egress asymmetry in the occultation profile, as we argue in the next section.

4.7. Scattering

The putative dust cloud likely attenuates more by scattering photons out of our line of sight than by actual absorption (this is due to the small imaginary part of the index of refraction in the visible; see, e.g., Denevi et al. 2007). This leaves open the possibility that at certain orbital phases, there could be an *excess* of light above the nominal out-of-occultation region levels. This would require the presence of some larger ($s \gtrsim 1 \mu\text{m}$) grains that scatter primarily in the forward direction.

We can estimate the ratio of fluxes scattered into, versus out of, our line of sight. Consider an idealized, small, spherical scattering cloud of radius R_d that scatters a fraction A (for “albedo”) of all the stellar radiation incident upon it (i.e., the cloud presents a total scattering cross section of $A \cdot \pi R_d^2$). The incident radiation is scattered uniformly into a solid angle Ω_{scat} centered about the direction of the incident beam. In the case that the cloud sits directly in front of the target star, the ratio of fluxes scattered into, versus out of, the line of sight is

$$\frac{\chi_{\text{in}}}{\chi_{\text{out}}} \simeq \frac{\pi}{\Omega_{\text{scat}}} \left(\frac{R_s}{a} \right)^2 \simeq \frac{\pi}{16 \Omega_{\text{scat}}} \quad (18)$$

independent of A and R_d . The ratio ranges from $\sim 1.6\%$ for isotropic scattering, to as high as $\sim 20\%$ for forward scattering into 1 steradian. If the dust cloud is blocking

the stellar disk, then attenuation is dominant (except in the case of extreme forward scattering). However, if the dust cloud is not blocking the stellar disk, then there may be a small excess contribution to the system light. This may provide an explanation for the small bump in flux just before ingress, followed by a small depression in the flux just after egress (see Fig. 3). The asymmetry results from the asymmetric distribution of the dust in the tail.

4.8. Tidal Inspiral Lifetime

We now consider how long such a planet as the one we are proposing might last in the face of tidal decay due to interactions with the parent star. The expression for the timescale of tidal decay is given by

$$\tau_{\text{tidal}} \simeq Q \frac{2M_s}{9M_p} \left(\frac{a}{R_s} \right)^5 \frac{P_{\text{orb}}}{2\pi} \simeq 10^{10} \left(\frac{Q}{10^6} \right) \text{ yr} \quad (19)$$

(see, e.g., Gu, Lin, & Bodenheimer 2003) where Q is the usual dimensionless measure of dissipation in the parent star, and we have assumed that the parent star is rotating with an angular frequency much smaller than the planet’s orbital frequency, and that the orbital eccentricity is zero. Thus, even for a pessimistically small value of Q , the lifetime against tidal decay is more than adequately long.

4.9. Differences Between KIC 12557548 and Hot Super-Earths

If our proposed scenario for KIC 1255b is correct, why don’t other hot rocky planets also evince occulting dust clouds? The class of close-in rocky planets includes CoRoT-7b (Leger et al. 2009; Leger et al. 2011), 55 Cnc e (Winn et al. 2011), and Kepler-10b (Batalha et al. 2011b).¹² All are argued to have significant rock components, although an admixture of water, hydrogen, and/or other light elements seems required to explain 55 Cnc e.

The primary parameter distinguishing the super-Mercury that we are imagining orbits KIC 12557548 and the other hot rocky planets is clearly the planet mass. All the other planets are “super-Earths” having masses $M_p \simeq 10 M_{\oplus}$ and radii $R_p \simeq 2 R_{\oplus}$ (for mass-radius relations for super-Earths, see, e.g., Valencia et al. 2007 or Figure 3 of Winn et al. 2011). Super-Earths have surface escape velocities of $v_{\text{esc,p}} \simeq 25 \text{ km/s}$, almost certainly too large for gas that is heated to temperatures $T \simeq 2000\text{--}3000 \text{ K}$ to escape at substantial rates via Parker-type winds. The efficiency of driving a thermal wind drops rapidly with increasing $v_{\text{esc,p}}$. The *local* hydrostatic scale height of gas (valid for altitudes smaller than R_p)

$$h \sim \frac{2c_s^2}{v_{\text{esc}}^2} R_p \sim 2 \times 10^{-3} \left(\frac{30}{\mu} \right) \left(\frac{10 M_{\oplus}}{M_p} \right) \left(\frac{R_p}{2 R_{\oplus}} \right) R_p \quad (20)$$

decreases as $1/v_{\text{esc}}^2$. Because the gas density depends exponentially on $1/h$, the base of a Parker-type wind in a super-Earth atmosphere (where the base is roughly identified as that location where the local value of $v_{\text{esc}}/c_s \sim 6$; for super-Earths this would lie several R_p away from

¹² Kepler-9d (Batalha et al. 2011a) may also belong to this class based on its size and orbital distance, but unfortunately the mass is not yet known, and therefore we cannot be sure that it is a purely rocky planet.

the planetary surface) would be many orders of magnitude less dense than the base of the wind on our super-Mercury (which sits near the first scale height of the planetary surface).

We expended some effort considering alternative mechanisms of mass loss from super-Earths: (i) XUV photoevaporation (by analogy with hot Jupiters), (ii) stellar wind drag, and (iii) stellar radiation pressure. All failed to reproduce the inferred mass loss rates for KIC 12557548. The intercepted power from the stellar XUV luminosity is at least a factor of 10 too low compared to L_{required} (see equation 15), even for optimistically high values of $L_{\text{XUV},s} = 10^{-5}L_{\odot}$ and of the efficiency $\varepsilon = 0.1$ with which XUV photon energy is converted to mechanical work.^{13,14} Stellar wind drag suffers the same problem that XUV photoevaporation does: the power intercepted by the planet from the stellar wind is insufficient to supply L_{required} . An easy way to see this is to note that the mechanical luminosity of the Solar wind is $L_{\text{wind},s} \sim (1/2)\dot{M}_{\odot}v_{\text{wind},s}^2 \sim (1/2) \cdot (2 \times 10^{-14}M_{\odot}/\text{yr}) \cdot (400\text{ km/s})^2 \sim 3 \times 10^{-7}L_{\odot} < L_{\text{XUV},s}$.^{15,16} The intercepted power is still too low even were we to account for a planetary magnetosphere, which would increase the cross section presented by the planet by a factor $\lesssim 10$.¹⁷ Finally, based on the calculations of Kimura et al. (2002), the force of stellar radiation pressure acting on a grain is at most $\sim 30\%$ of the force of planetary gravity on a super-Earth, for conditions in KIC 12557548 (but see §§4.6–4.7 where we saw that once grains escape the planet, stellar radiation pressure shapes the dust tail in ways that can explain certain features of the occultation profile). Moreover, even if the force of radiation pressure on a grain were somewhat larger than that of planetary gravity, the grain would be dragged on by ambient gas, and may never accelerate to escape velocity.

For all these reasons, super-Earths cannot launch dusty outflows like those we infer for KIC 12557548—whereas sub-Earths can. There is still another reason why dust clouds are especially observable for KIC 12557548 and not in the other observed systems. Even if dust grains could be driven off the hot super-Earths detected to date, they would be too hot; grains in these other systems would sublimate too quickly to travel far from their parent planets, and would fail to block as much light from their host stars. If we use equation (4) to estimate the temperature of a grain at the location of each super-Earth, we find:

- Kepler-10b : 3000 K

¹³ XUV luminosities of K dwarfs are typically $3 \times$ greater than those of G dwarfs (Hodgkin & Pyle 1994; Lecavelier des Etangs 2007).

¹⁴ The efficiency ε is lowered by ionization and radiative losses; radiative losses may be especially severe in the case of KIC 1255b because of cooling by dust, a problem that does not seem to afflict hot Jupiter winds.

¹⁵ Mass loss rates of K stars are observed to be comparable to that of the Sun (Wood et al. 2005; Cranmer 2008).

¹⁶ At the orbital distance of KIC 1255b, the energy carried by the stellar wind is mostly magnetic and thermal, not kinetic. But after accounting for all three forms of energy using empirical measurements of the Solar wind at $a = 2.8R_{\odot}$, we arrived at roughly the same total power output, $L_{\text{wind},s} \sim 10^{-6}L_{\odot}$.

¹⁷ If KIC 1255b has a surface dipole field of 1 G, then its magnetospheric radius is $\sim 2R_p$.

- 55 Cnc e : 2800 K
- CoRoT-7b : 2500 K
- KIC 1255b : 2100 K

Thus KIC 1255b—orbiting the coolest star—is distinguished in having the coolest grains. Sublimation lifetimes t_{sub} are exponentially sensitive to temperature. For example, whereas we have estimated $t_{\text{sub}} \sim 3 \times 10^4$ s for $0.2\text{-}\mu\text{m}$ -sized pyroxene grains emitted by KIC 1255b, these same grains emitted by CoRoT-7b would have $t_{\text{sub}} \sim 10^2$ s (Kimura et al. 2002)—considerably shorter than the travel time $t_{\text{travel}} \sim 2 \times 10^4$ s required to produce a $\sim 1\%$ occultation (§4.2).

Thus KIC 1255b apparently occupies a sweet spot for the production of occulting dust clouds: the system is hot enough for surface silicates to vaporize and emit dust, but cool enough that these dust particles can travel a significant fraction of the host stellar radius.

5. SUMMARY AND OUTLOOK

In this work we have reported a periodically occurring set of occultations in the light of KIC 12557548 with a period of 15.6854 hours. The depths of these occultations range from 1.2% to $\lesssim 0.15\%$, and vary on timescales comparable to, if not also shorter than, the occultation period. A search for periodic modulation in the depths of the occultations did not reveal anything definitive. From various lines of evidence, most notably our own optical spectrum, the target star appears to be a mid-K dwarf.

We briefly considered a scenario wherein the changing transit depths are due to a dual giant planet system (either on separate orbits or in a binary pair) in which one of the planets undergoes grazing transits of the target K star. The orbital plane of the transiting planet would have to precess in such a way as to effect the variable occultation depths. We find, however, that a binary planet configuration is very likely to be dynamically unstable, even if the two planets are themselves essentially in a contact configuration. In the case of two planets on separate orbits, it is not clear how orbital precession could explain either the remarkably fast variability on orbital timescales or the long intervals of ~ 10 and 20 days when the occultations mostly disappear.

We come down in favor of a scenario in which dust is aerodynamically dragged off an orbiting rocky planet—possibly one not much larger than Mercury in size—by a thermal Parker-type wind composed of metal atoms sublimated off the planet’s surface at a temperature of ~ 2000 K. At maximum eclipse depth, the mass loss rate is on the order of a few times 10^{11} g/s, or about $1M_{\oplus}/\text{Gyr}$, possibly in roughly equal parts gas and dust by mass. Our fiducial mass and radius for the underlying planet are $0.1M_{\oplus}$ and $0.5R_{\oplus}$, respectively. The corresponding lifetime against evaporation is ~ 0.2 Gyr. This is probably less than the age of the star, but not alarmingly so. Because the mass loss rates are inferred from the observations and as such are largely fixed, planets much smaller in mass than our fiducial super-Mercury have implausibly short evaporation lifetimes. And planets much larger in mass than our fiducial super-Mercury run into the severe theoretical problem of understanding how gas and dust could flow off their high-gravity surfaces at the rates mandated by observation.

Upon being accelerated out of the planet's gravity well by gas pressure, dusty gas should become sufficiently rarefied that the dust and gas decouple. We have simulated how dust grains, decoupled from gas, would be shaped into a comet-like tail by the Coriolis force and stellar radiation pressure. The head-tail asymmetry of the dust cloud promises to explain an observed ingress-egress asymmetry in the occultation profile. Pyroxene grains, each a fraction of a micron in size, are a good candidate for the obscuring grains because of their relatively long lifetimes against sublimation (\gtrsim hours), even within a few stellar radii of the parent star. The temporal variability of the occultation depths would be explained by a time-varying density in the outgoing dust flow, caused perhaps by irregularities and uneven outgassing rates in the planet's surface; a feedback cycle between mass loss and the stellar radiation flux received at the planet's surface that causes both to fluctuate with time; and/or instabilities resulting from the interaction of the ionized planetary wind with the magnetized stellar wind. The analogy between our evaporating super-Mercury and comets is a close one.

5.1. Observational Prospects

Obviously, short-cadence observations with *Kepler* would be helpful in clarifying the issue of whether there are shape changes in individual occultations vs. only changes in the overall depths. The target star, at $K_p = 15.7$ magnitudes, is not very bright, but we estimate that each 1-minute sample of a short-cadence observation with *Kepler* would yield 0.15% counting statistics. Given that the depths of the deepest occultations are 1.2%, this would provide a signal-to-noise of 8:1 for individual samples. With greater time resolution and sensitivity, one can look for stronger evidence of ingress-egress asymmetries that would speak to the comet-tail morphology of the dusty outflow.

Ground-based observations with a large optical/infrared telescope might also prove helpful. Broadband photometry from the optical through the infrared would give eclipse depths as a function of wavelength and thereby constrain dust particle sizes. The detection of solid-state absorption features (e.g., the 10 μm silicate band) would confirm the presence of dust.

Finally, spectral observations with the *Hubble Space Telescope* searching for absorption line features of metals—e.g., photoionized Mg, O, Si, Ca, and Fe, and perhaps also Na (see Schaefer & Fegley 2009)—during occultations could lead to a direct demonstration that the underlying planet is comprised largely of heavy elements, and secure our hypothesis that it is emitting a wind (cf. Linsky et al. 2010).

If there indeed turns out to be a super-Mercury orbiting KIC 12557548, where the occultations are due to dust carried by outflowing sublimated gas, this would be (i) the smallest-mass extrasolar planet ever to have been (indirectly) detected, and (ii) the first planet shown to be disintegrating via the loss of macroscopic particles, emitted from an atmosphere composed largely of high-Z material.

Manga for instructive exchanges about vaporizing silicates and volcano ejecta speeds, and Josh Carter for discussions about data validations and the viability of a dynamically stable binary planet. We consulted with Ron Remillard, Rob Simcoe, and Adam Burgasser about spectral classifications. We would also like to thank Robert Lamontagne and the staff at the Observatoire Astronomique du Mont-Mégantic for their assistance. EC is grateful for support from the National Science Foundation. LN thanks the Natural Sciences and Engineering Research Council (NSERC) of Canada for financial support. BK is grateful to the MIT Kavli Institute for Astrophysics and Space Research for the hospitality they extended during her visit and the support provided by the Turkish Council of Higher Education.

REFERENCES

- Agol, E., Steffen, J., Sari, R., & Clarkson, W. 2005, *MNRAS*, 359, 567
- Batalha, N., et al. 2010, *ApJ*, 713, L10
- Batalha, N., et al. 2011a, *ApJ*, 727, 24
- Batalha, N., et al. 2011b, *ApJ*, 729, 27
- Batygin, K., Stevenson, D.J., & Bodenheimer, P.H. 2011, *ApJ*, 738, 1
- Ben-Jaffel, L. 2008, *ApJ*, 688, 1352
- Borucki, W. J., et al. 2011, *ApJ*, 736, 19
- Burns, J.A., Lamy, P.L., & Soter, S. 1979, *Icarus*, 40, 1
- Castan, T. & Menou, K. 2011, *ApJ*, 743, 36
- Cranmer, S.R. 2008, *ASP Conference Series*, 14th Cambridge Workshop on Cool Stars, Stellar Systems, and the Sun, 384, 317
- Dawson, R.I., & Fabrycky, D.C. *ApJ*, 2010, 722, 937
- Delsemme, A.H. 1982, *Icarus*, 49, 438
- Deveni, B.W., Lucey, P.G., Hochberg, E.J., & Steutel, D. 2007, *JGR*, 112, E05009
- Epstein, P.S. 1924, *Physical Review*, 23, 710
- Fernandez, J.A. 2005, *Comets: Nature, Dynamics, Origin, and Their Cosmogonical Relevance*, (Springer Science & Business)
- Fischer, D.A., et al. 2008, *ApJ*, 675, 790
- García-Muñoz, A. 2007, *P&SS*, 55, 1426
- Gu, P.-G., Bodenheimer, P.H., & Lin, D.C. 2003b, *ApJ*, 588, 509
- Lamers, H.J.G.L.M., & Cassinelli, J.P. 1999, *Introduction to Stellar Winds*, (Cambridge, UK: Cambridge University Press)
- Lecavelier des Etangs, A. 2007, in *UV Astronomy: Stars from Birth to Death*, Proceedings of the UASB Conference, eds. A.I. Gomez, de Castro & M.A. Barstow
- Hansen, B.M.S., & Murray, N. 2011, *arXiv:1105.2050*
- Harrington, R.S. 1972, *Cel. Mech.*, 6, 322
- Hodgkin, S.T., & Pye, J.P. 1994, *MNRAS*, 267, 840
- Holman, M., & Murray, N. 2005, *Science*, 307, 1288
- Hsieh, H.H., Jewitt, D., Lacerda, P., Lowry, S.C., & Snodgrass, C. 2010, *MNRAS*, 403, 363
- Jacoby, G.H., Hunter, D.A., & Christian, C.A. 1984, *ApJ Supp.*, 56, 257
- Jaschek, C. & Jaschek, M. 1987, "The Classification of Stars", Cambridge Univ. Press, Cambridge
- Jenkins et al. 2010, *ApJ*, 724, 1108
- Jewitt, D. 1996, *Earth, Moon, and Planets*, 72, 185
- Kimura, H., Mann, I., Biesecker, D.A., & Jessberger, E. K. 2002, *Icarus*, 159, 529
- Kotson, M., Rappaport, S., & Levine, A. 2012, in preparation.
- Lecavelier des Etangs, A. 2007, *A&A*, 461, 1185
- Lecavelier des Etangs, A., et al. 2010, *A&A*, 514, 72
- Léger, A., et al. 2009, *A&A*, 506, 287
- Léger, A., et al. 2011, *Icarus*, 312, 1
- Lemaire, J.F. 2011, *arXiv:1112.3850*
- Linsky, J.L., Yang, H., France, K., Froning, C.S., Green, J.C., Stocke, J.T., & Osterman, S.N. 2010, *ApJ*, 717, 1291
- Mikkola, S. 2008, *Multiple Stars Across the H-R Diagram*, ESO Astrophysics Symposia, Volume . ISBN 978-3-540-74744-4. Springer-Verlag Berlin Heidelberg, 2008, p. 11
- Muirhead, P.S., et al. 2012, *ApJ*, in press, *arXiv:1201.2189*
- Murray-Clay, R., Chiang, E., & Murray, N. 2009, *ApJ*, 693, 23
- Podsiadlowski, Ph., Rappaport, S., Fregeau, J., & Mardling, R. 2010, *arXiv:1007.1418*
- Prsa, A., et al. 2011, *AJ*, 141, 83
- Rauer, H. 2007, in *Trans-Neptunian Objects and Comets*, Saas-Fee Advanced Courses, 35, 165

We thank Edwin Kite, Raymond Jeanloz, and Michael

- Schaefer, L. & Fegley, B., Jr 2009, *ApJ*, 703, L113
Schaefer, L. Lodders, K., & Fegley, B., Jr 2011, arXiv:1108.4660
Valencia, D., Sasselov, D.D., & O'Connell, R.J. 2007, *ApJ*, 665, 1413
Vidal-Madjar, A., Désert, J.-M., Lecavelier des Etangs, A., et al. 2003, *Nature*, 422, 143
Windhorst, R.A., et al. 1991, 380, 362
Winn, J. N., et al. 2011, *ApJ Lett.*, 737, 18
Wood, B.E., Müller, H.-R., Zank, G.P., Linsky, J.L., & Redfield, S. 2005, *ApJ*, 628, L143
Yelle, R.V. 2004, *Icarus*, 167, 30